Tuberculosis 95 (2015) 60–67

Contents lists available at ScienceDirect

Tuberculosis

journal homepage: http://intl.elsevierhealth.com/journals/tube

BOVINE TUBERCULOSIS

MicroRNA profiling of the bovine alveolar macrophage response to *Mycobacterium bovis* infection suggests pathogen survival is enhanced by microRNA regulation of endocytosis and lysosome trafficking

Peter Vegh [a, b], David A. Magee [c, 2], Nicolas C. Nalpas [c], Kenneth Bryan [a], Matthew S. McCabe [a], John A. Browne [c], Kevin M. Conlon [d], Stephen V. Gordon [d, e], Daniel G. Bradley [b], David E. MacHugh [c, e], David J. Lynn [a, *, 1]

[a] *Animal & Bioscience Research Department, Animal & Grassland Research and Innovation Centre, Teagasc, Grange, Dunsany, Co. Meath, Ireland*
[b] *Smurfit Institute of Genetics, Trinity College, Dublin 2, Ireland*
[c] *Animal Genomics Laboratory, UCD School of Agriculture and Food Science, UCD College of Agriculture, Food Science and Veterinary Medicine, University College Dublin, Belfield, Dublin 4, Ireland*
[d] *UCD School of Veterinary Medicine, UCD College of Agriculture, Food Science and Veterinary Medicine, University College Dublin, Belfield, Dublin 4, Ireland*
[e] *UCD Conway Institute of Biomolecular and Biomedical Research, University College Dublin, Belfield, Dublin 4, Ireland*

ARTICLE INFO

Article history:
Received 6 August 2014
Received in revised form
16 October 2014
Accepted 28 October 2014

Keywords:
Bos taurus
Alveolar macrophage
microRNA
RNA-seq
Mycobacterium bovis
Tuberculosis

SUMMARY

Mycobacterium bovis, the causative agent of bovine tuberculosis, a major problem for global agriculture, spreads via an airborne route and is taken up by alveolar macrophages (AM) in the lung. Here, we describe the first next-generation sequencing (RNA-seq) approach to temporally profile miRNA expression in primary bovine AMs post-infection with *M. bovis*. One, six, and forty miRNAs were identified as significantly differentially expressed at 2, 24 and 48 h post-infection, respectively. The differential expression of three miRNAs (bta-miR-142-5p, bta-miR-146a, and bta-miR-423-3p) was confirmed by RT-qPCR. Pathway analysis of the predicted mRNA targets of differentially expressed miRNAs suggests that these miRNAs preferentially target several pathways that are functionally relevant for mycobacterial pathogenesis, including endocytosis and lysosome trafficking, IL-1 signalling and the TGF-β pathway. Over-expression studies using a bovine macrophage cell-line (Bomac) reveal the targeting of two key genes in the innate immune response to *M. bovis*, IL-1 receptor-associated kinase 1 *(IRAK1)* and TGF-β receptor 2 *(TGFBR2)*, by miR-146. Taken together, our study suggests that miRNAs play a key role in tuning the complex interplay between *M. bovis* survival strategies and the host immune response.

1. Introduction

Tuberculosis (TB) is a major global health threat to both human and animal populations, which is caused by members of the intracellular *Mycobacterium* genus. Currently, one third of the human population world-wide is estimated to be infected with *Mycobacterium tuberculosis*, causing approximately nine million new cases and 1.3 million deaths every year [1]. Bovine tuberculosis, caused by *Mycobacterium bovis*, is also a significant problem for global agriculture. Both *M. tuberculosis* and *M. bovis* are members of the *M. tuberculosis* complex (MTBC), a group of highly related pathogens that are spread via an airborne route and are taken up by alveolar macrophages (AM) in their respective hosts. It is well established that *M. tuberculosis* and *M. bovis* can block the antimicrobial systems of the macrophage allowing them to replicate intracellularly and cause disease [2]. There is increasing evidence for the role of the innate immune response in the outcome of MTBC pathogens [3]. Macrophages are the first cells to encounter mycobacteria, and microarray [4] and RNA-seq experiments [5] have shown that mRNA expression is substantially altered in bovine monocyte-derived macrophages (MDM) upon *M. bovis* infection *in vitro*. Changes in the expression of another type of RNA, microRNAs, however, are less well understood. MicroRNAs (miRNAs) are short non-coding RNAs that post-transcriptionally regulate gene expression [6] and are known to have roles in many

* Corresponding author. South Australian Health and Medical Research Institute, North Terrace, Adelaide, SA 5000, Australia. Tel.: +61 881 284 053.
E-mail address: david.lynn@sahmri.com (D.J. Lynn).
[1] Current address: School of Medicine, Flinders University, PO Box 11060, Adelaide, SA 5001, Australia.
[2] Current address: Department of Animal Science, University of Connecticut, Storrs, CT, USA.

http://dx.doi.org/10.1016/j.tube.2014.10.011

aspects of immunity [7]. Several miRNAs have been found to be involved in mycobacterial infection [8]. In mice infected with the vaccine strain *M. bovis* BCG, downregulated miR-29 expression in natural killer cells and T cells enhanced IFN-γ production, a cytokine important for immunity against intracellular pathogens [9]. Similarly, in human MDMs infected with *Mycobacterium avium*, caspase 3 and 7 are downregulated by miRNAs let-7e and miR-29a, thus inhibiting apoptosis, a defense mechanism against intracellular bacteria [10].

In this paper, we have built upon our previous work profiling miRNA expression in bovine AM using RNA-seq [11], and investigate which miRNAs are differentially expressed in primary bovine AM at several time-points post-infection with the genome-sequenced strain of *M. bovis* 2122/97 in comparison to paired uninfected controls.

2. Materials and methods

2.1. Animals

Ten unrelated age-matched (7–12 weeks) Holstein–Friesian male calves were used in the challenge experiment. All animals were maintained under uniform housing conditions and nutritional regimens at the UCD Lyons Research Farm (Newcastle, County Kildare, Ireland). The animals were selected from a herd without a recent history of bovine tuberculosis infection.

2.2. Alveolar macrophage in vitro infection

AM were harvested by pulmonary lavage of lungs obtained post-mortem from ten animals, and collected in cryovials as described before by Magee et al. (2014). The cryovials, containing 2.5×10^7 AM cells in 1 mL, were stored at −80 °C for a period of 20 h after which they were removed from the freezing containers and transferred to −140 °C freezer storage conditions until further use [12].

Alveolar macrophage culture was prepared as described by Magee et al. (2014). Briefly, cryovials were thawed by placing in a 37 °C water bath for 1 min. Once thawed, cells were immediately transferred into 20 ml 37 °C pre-warmed R10+ media (RPMI 1640 medium [Invitrogen, Life Technologies Ltd., Paisley, UK], supplemented with 10% fetal bovine serum [FBS; Sigma–Aldrich, Dublin, Ireland], [Sigma–Aldrich], 2 mM L-glutamine [Sigma–Aldrich], 100 μg/ml ampicillin [Sigma–Aldrich] and 25 μg/ml gentamycin [Sigma–Aldrich]) and centrifuged ($200 \times g$ for 5 min). The cell pellet was resuspended in 15 ml of R10+ media and placed in a 75 cm^2 vented culture flask (CELLSTAR Greiner Bio-One Ltd., Stonehouse, UK), and incubated for 24 h at 37 °C, 5% CO_2. After incubation, alveolar macrophages were seeded in 24-flat well tissue culture plates (Sarstedt Ltd.) at a density of 5×10^5 cells/well, and incubated for a further 24 h at 37 °C, 5% CO_2. Separate infected and control wells were maintained for each of the 4 time points (2 h, 6 h, 24 h, 48 h), in addition to the control (0 h). All *in vitro* infections were performed in a CL3 laboratory. For this, the media from all wells was removed and replaced with 1 ml R10 media containing *M. bovis* (5×10^6 cells/ml). The non-infected control alveolar macrophage samples received 1 ml R10 media only. After infection, the tissue culture plates were incubated at 37 °C, 5% CO_2 for 24 h and 48 h. After 2 h infection, the media from all wells of the 24 h and 48 h infection experiments was replaced with fresh R10 media (1 ml per well) and the plates were re-incubated at 37 °C, 5% CO_2 until the cells were harvested [12]. Two samples (48 h infected and control for animal N1861) were excluded due to low cell numbers, therefore nine animals were used in the 48 h timepoint.

2.3. Small RNA preparation

In total, 88 RNA-seq libraries were prepared for sequencing. The small and total RNA fractions were prepared from the cells using the RNeasy Plus Mini kit and RNeasy MinElute Cleanup Kit (Qiagen Ltd., Manchester, UK), according to Appendix E of the manufacturer's protocol. The quality and quantity of the prepared total and small RNA were assessed using the 6000 Nano and small RNA LabChip kits (Agilent Technologies Ireland Ltd., Cork, Ireland) with an Agilent 2100 Bioanalyzer (Agilent Technologies Ireland Ltd.). The total RNA fractions had RIN values between 8.6 and 9.5. Small RNA concentrations were between 3400 and 17,200 pg/μl, and miRNA concentrations were between 140 and 1430 pg/μl (Supplementary Table 1). The small RNA fractions were used for preparing RNA-seq libraries and for RT-qPCR.

2.4. RNA-seq library preparation

All 88 RNA-seq libraries were prepared with the Illumina Truseq Small RNA Sample Preparation Kit (Illumina Inc., Madison, WI, USA), according to the manufacturer's protocol, using 5 μl of the prepared small RNA. Libraries were sequenced (50 bp single-end) on 18 lanes of an Illumina HiSeq 2000 machine (BGI Hong Kong, China). The RNA-seq fastq files have been uploaded to the NCBI Gene Expression Omnibus (GEO) database [13] with experiment series accession number GSE58883.

2.5. Analysis of RNA-seq data

Sample quality and read numbers were assessed using FASTQC (v0.10.0, http://www.bioinformatics.bbsrc.ac.uk/projects/fastqc/). Cutadapt (v1.2.1) [14] was used to trim 3′ adapter sequences from reads. Reads that were less than 18 nucleotides (nt) after trimming, and all untrimmed reads were discarded. The remaining reads were then further filtered using FASTQ Quality Filter (FASTX Toolkit v0.0.13.2, http://hannonlab.cshl.edu/fastx_toolkit/). Reads where more than 30% of the bases had a Phred score <20 were removed. Finally, reads passing all the above filters were also trimmed at their ends using FASTQ Quality Trimmer (FASTX Toolkit v0.0.13.2) to remove low quality bases (Phred score < 20), and reads less than 18 nt after the trimming were discarded. Reads that passed all quality control steps were aligned to the bovine genome (UMD3.1 assembly [15]) using Novoalign (Novocraft Technologies, v2.08.03) in 'miRNA' mode, allowing one mismatch. Non-uniquely aligning reads were discarded. HTSeq-count (part of the HTSeq framework, v0.5.3p3) in 'union' mode was then used to count aligned reads that overlapped with known miRBase (version 19, http://www.mirbase.org) [16] miRNA gene annotations. To investigate the proportion of reads sequenced from non-miRNA genes, HTSeq-count was also used separately to count reads that overlapped with all bovine gene annotations from Ensembl version 69. For a summary of the number of reads at each step, see Supplementary Table 1.

Potentially novel miRNAs were identified using miRDeep2 (v2.0.0.5) [17]. The predicted novel miRNAs that were independently predicted in at least three samples and fulfilled all of the following criteria were submitted to miRBase: the mature sequence was expressed in at least ten samples and was expressed at a minimum of 100 reads per million (RPM); the predicted miRNA had a high (>90%) probability of being a true miRNA according to miRDeep2; and the hairpin structure had a RandFold *P* value <0.05.

R (v3.0.1, http://www.r-project.org) was used to create the boxplots and the scatter plots. EdgeR (v3.2.4) [18] was used to identify statistically significant differentially expressed miRNAs with a paired test, using a generalized linear model (glm) method, with upper quartile normalization [19]. Differentially expressed

miRNAs were defined as those that had both an FDR ≤0.05 in the edgeR analysis and were expressed above a threshold of 100 RPM, a level at which miRNAs are more likely to be functional [20]. Results were robust for the normalization method used: all differentially expressed miRNAs were also detected with the other two normalization methods; TMM (trimmed mean of M-values) and RLE (relative log expression).

2.6. Co-expression and target analysis of miRNA and mRNA data

To identify mRNAs that were potentially regulated by differentially expressed (DE) miRNAs, Pearson correlations were calculated between DE miRNA expression and mRNA expression (also assayed by RNA-seq) from the same samples (Nalpas et al., manuscript submitted) using the Apache Commons Java Statistics Library (http://commons.apache.org/proper/commons-math). The resulting correlation matrix was then filtered to remove both non-significant correlations (critical value for Pearson's correlation for this matrix is $r = -0.2483$) and those inverse correlations that were not supported by miRanda (v3.3a) predicted miRNA-target pairs. Two-dimensional cluster analysis and visualization, using R (v3.0.1) *hclust* and *heatmap.plus* packages, was then applied to the filtered correlation matrix. The miRNA-mRNA interaction network was also visualized with Cytoscape (v3.0.0) [21].

2.7. Pathway analysis of predicted miRNA target genes

The predicted target gene IDs of differentially expressed miRNAs were converted using 1:1 orthology annotation to human gene IDs and submitted to InnateDB [22] for pathway analysis. Genes were submitted in two groups; those that were targets of upregulated miRNAs, and those that were targets of downregulated miRNAs. Significant pathways were identified using the Hypergeometric test and were defined as having a Benjamini and Hochberg corrected *P* value of ≤0.05 [23].

2.8. RT-qPCR validation of differentially expressed miRNA genes

The expression of four miRNAs identified as differentially expressed in the RNA-seq data (bta-miR-22, bta-miR-142-5p, bta-miR-146a, and bta-miR-423-3p) was investigated using reverse transcription quantitative real time PCR (RT-qPCR). Infected and control samples were compared for nine biological replicates. Based on the RNA-seq data, bta-miR-16b and bta-miR-26b were used as non-differentially expressed internal reference transcripts.

The Taqman MicroRNA Reverse Transcription Kit (Applied Biosystems, Life Technologies Ltd., Warrington, UK) was used, according to the manufacturer's protocol, and using 5 μl of 10 × diluted small RNA fraction, in 15 μl reverse transcription reaction (30 min 16 °C, 30 min 42 °C, 5 min at 85 °C, and then maintained at 4 °C). Taqman MicroRNA Assays (Applied Biosystems) with TaqMan Universal Master Mix II (no UNG) (Applied Biosystems), were used according to the manufacturer's protocol.

A 7500 Fast Real-Time PCR System (Applied Biosystems, software version 2.0.6) was used with MicroAmp Fast optical 96-well plates and Optical Adhesive Films (Applied Biosystems). Amplification was performed using 20 μl/well and the following thermal cycle: 95 °C 10 min, and 40 cycles: 95 °C for 15 s, 60 °C for 1 min. Technical replication was performed in triplicate and results were corrected for amplification efficiency. No amplification was measured in the no template and the reverse transcription control wells. The one-tailed paired Student's *t*-test was performed with R (v3.0.1) on the normalized and efficiency-corrected ΔC_t (quantification cycle) values, with a significance level of 0.05. Using the Pfaffl method [24], fold changes were calculated from the $\Delta\Delta C_t$ values ($FC = 2^{-\Delta\Delta Ct}$), using the negative reciprocal for down-regulated genes (−1/FC).

2.9. Transfection of Bomac cells with miRNA mimics

Bomac cells were a gift from Prof. Cliona O'Farrelly (Trinity College Dublin). Although Bomacs poorly replicate all the functions

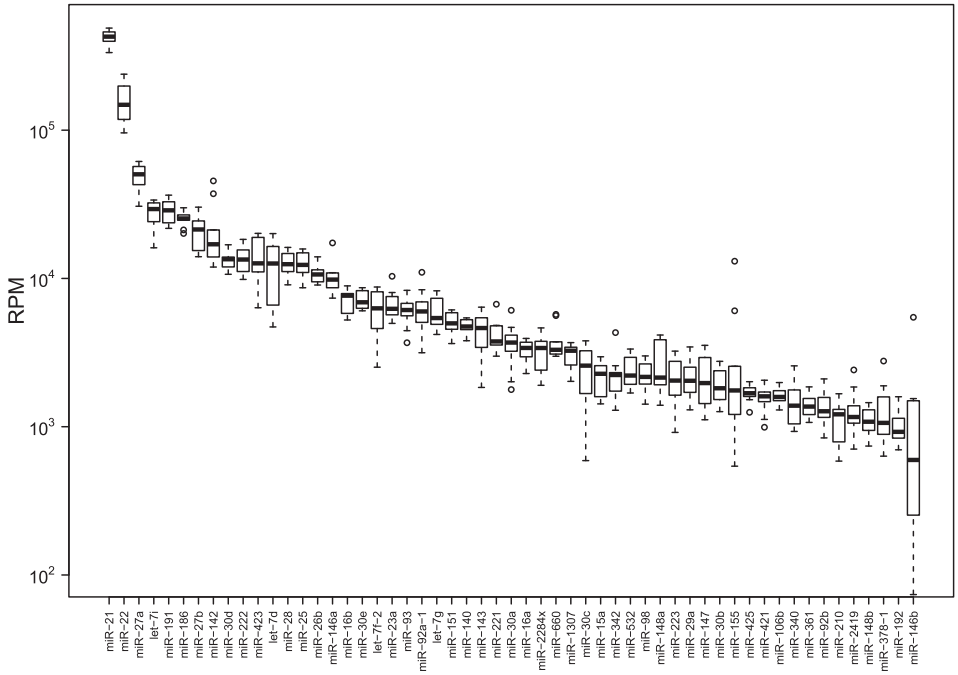

Figure 1. MicroRNA expression in unchallenged bovine alveolar macrophages. Only those expressed above a threshold of 1000 RPM are shown.

of primary macrophages [25], the Bomac cell-line is, to our knowledge, the only bovine macrophage cell-line available to undertake the miRNA mimic transfection studies and these experiments are largely independent of these functions. Cells were cultured in 150 cm^2 flasks (CELLSTAR Greiner Bio-One) using RPMI 1640 medium (Sigma–Aldrich), supplemented with 10% FBS (Sigma–Aldrich), Penicillin (50 unit/ml) and Streptomycin (50 μg/ml) (Pen Strep, Gibco, Life Technologies). For the transfection, cells were seeded in 6 well flat bottom cell culture plates (CELLSTAR Greiner Bio-One). Cells were transfected using Opti-MEM 1 (Gibco, Life Technologies) and Lipofectamine RNAiMAX (Invitrogen, Life Technologies), according to the manufacturer's protocol and using 75 pmol mimics (Ambion mirVana miRNA mimics, Life Technologies) per well. Based on the RNA-seq and RT-qPCR results, miR-146a and miR-146b were selected for the experiment. Additional wells were treated with negative (scrambled) control mimic, or the positive control (miR-1). Each well was treated with one miRNA only. As per the manufacturer's recommendation, downregulation of miR-1's known target, *PTK-9,* was measured to confirm that transfection was successful. Experiments were performed in triplicate. After 24 h, cells were washed with PBS (pH 7.4, Gibco, Life Technologies) and then cells were lysed with the Ambion mirVana miRNA Isolation Kit (Life Technologies). Total RNA was quantified with a Nanodrop ND-1000 and an Agilent 2100 Bioanalyzer, and all samples had RIN values above 9, and 28S/18S rRNA ratios between 1.8 and 2.3.

2.10. RT-qPCR analysis of target gene downregulation

The expression of two bovine genes, IL-1 receptor-associated kinase 1 *(IRAK1)* and TGF-β receptor 2 *(TGFBR2),* was measured with RT-qPCR. Five genes, *ACTB, GAPDH, H3F3A, PPIA* and *RPS9,* were tested to find suitable internal reference genes. Three reference genes *(GAPDH, H3F3A, RPS9)* were selected with the Genorm algorithm [26], using the ReadqPCR and NormqPCR (version 1.8.0) R packages [27]. The High-Capacity cDNA Reverse Transcription Kit (Invitrogen, Life Technologies) was used, with 400 ng RNA in 20 μl reverse transcription reaction (10 min 25 °C, 120 min 37 °C, 5 min at 85 °C, and then maintained at 4 °C). The Fast SYBR Green Master Mix (Applied Biosystems) was used for assaying, using 1 μl of the cDNA. A 7500 Fast Real-Time PCR System was used as described above, using the following thermal cycling: 95 °C 20 s, and 40 cycles: 95 °C for 3 s, 60 °C for 30 s. The no-template and reverse transcription control showed that preparations were free of contamination. For primer sequences see Supplementary Table 2. Melt curve analysis confirmed specificity of primers. Treatments were compared to the scrambled mimic negative control. The two-tailed two-sample Student's *t*-test was performed on the normalized and efficiency-corrected ΔC_t values, with a significance level of 0.05. For the C_t values processed by NormqPCR, please see Supplementary Table 3. Fold changes were calculated using the Pfaffl method, as described above.

3. Results

A high-throughput sequencing approach was applied to monitor miRNA expression changes in bovine AM post-infection with *M. bovis* and in matched unchallenged control samples. In total, 2.5 billion reads were generated by sequencing, and approximately 2 billion reads remained for analysis after adapter removal and quality control. 93% of reads uniquely aligning to the genome aligned to annotated miRNAs in the bovine genome, 3.5% to small nucleolar RNAs (snoRNAs), and the remainder mapped mainly to other types of RNAs (mRNAs, tRNAs, rRNAs, mtRNAs etc). miRNA expression was highly correlated across biological replicates (Supplementary Figure 1). The most highly expressed miRNAs in unchallenged macrophages were bta-miR-21, bta-miR-22, bta-miR-27a, bta-let-7i and bta-miR-191 (Figure 1). The level of miRNA expression, however, varied over a wide range, with almost half of the reads aligning to bta-miR-21 (≈430,000 RPM), and the majority being more lowly expressed (1000–10,000 RPM). For a full list of the read counts for all miRNAs at all time-points, see Supplementary Table 4.

3.1. Multiple differentially expressed miRNAs were detected at 2, 24, and 48 hpi with M. bovis

The edgeR statistical package was used to determine miRNAs that were differentially expressed in response to *M. bovis* infection at 2, 6, 24, and 48 hpi. Only one miRNA, bta-miR-326, was identified

Table 1
Differentially expressed microRNAs in alveolar macrophages challenged with *M. bovis*. The results are sorted by time-point and fold-change.

miRNA	FC	RPM	*P* value	FDR
2 h post infection				
bta-miR-326	1.91	217.2	6.54×10^{-9}	2.09×10^{-6}
24 h post infection				
bta-miR-149-5p	1.81	284.4	2.21×10^{-4}	1.15×10^{-2}
bta-miR-27a-5p	1.53	390.5	1.18×10^{-3}	2.94×10^{-2}
bta-miR-21-3p	1.52	7735.2	1.09×10^{-3}	2.94×10^{-2}
bta-miR-147	1.51	2332.4	8.22×10^{-4}	2.66×10^{-2}
bta-miR-146a	1.47	13481.5	1.00×10^{-3}	2.94×10^{-2}
bta-miR-296	−1.79	132	6.21×10^{-5}	5.03×10^{-3}
48 h post infection				
bta-miR-146b	2.69	1526.5	3.95×10^{-6}	7.46×10^{-5}
bta-miR-146a	2.38	14030	7.36×10^{-9}	2.73×10^{-7}
bta-miR-147	2.17	2134.7	1.15×10^{-7}	3.84×10^{-6}
bta-miR-29c	2.12	381.3	1.35×10^{-6}	3.23×10^{-5}
bta-miR-22-3p/bta-miR-3600	1.96	152949.7	1.35×10^{-6}	3.23×10^{-5}
bta-miR-21-3p	1.79	5205.7	6.11×10^{-4}	4.30×10^{-3}
bta-miR-142-5p	1.76	15683.4	2.92×10^{-5}	4.65×10^{-4}
bta-miR-210	1.73	1324.4	3.70×10^{-4}	3.20×10^{-3}
bta-miR-32	1.69	604.6	1.34×10^{-4}	1.66×10^{-3}
bta-miR-125a	1.66	1824.2	8.30×10^{-4}	5.65×10^{-3}
bta-miR-155	1.65	3165.9	1.89×10^{-4}	2.11×10^{-3}
bta-miR-99b	1.63	1326.8	4.72×10^{-4}	3.50×10^{-3}
bta-miR-27a-5p	1.63	358.7	4.51×10^{-4}	3.43×10^{-3}
bta-miR-149-5p	1.61	366	3.01×10^{-4}	2.81×10^{-3}
bta-miR-28	1.6	1845.6	2.33×10^{-4}	2.43×10^{-3}
bta-miR-15a	1.54	1626.3	3.73×10^{-4}	3.20×10^{-3}
bta-miR-23a	1.51	5730.4	3.03×10^{-4}	2.81×10^{-3}
bta-miR-29a	1.49	1627.1	2.88×10^{-3}	1.66×10^{-2}
bta-miR-30b-5p	1.47	1671.1	4.06×10^{-3}	2.08×10^{-2}
bta-miR-151-5p	1.37	2640.2	5.83×10^{-3}	2.86×10^{-2}
bta-miR-92a	−1.36	6255.2	9.62×10^{-3}	4.07×10^{-2}
bta-let-7d	−1.43	12062.2	8.21×10^{-3}	3.61×10^{-2}
bta-miR-34a	−1.45	479.8	3.71×10^{-3}	1.97×10^{-2}
bta-let-7f	−1.46	7929	6.79×10^{-3}	3.19×10^{-2}
bta-miR-6529	−1.52	4179.4	2.18×10^{-3}	1.33×10^{-2}
bta-miR-107	−1.52	273.8	9.86×10^{-4}	6.46×10^{-3}
bta-miR-744	−1.55	330.4	4.21×10^{-4}	3.43×10^{-3}
bta-miR-328	−1.57	229.7	2.96×10^{-3}	1.68×10^{-2}
bta-let-7a	−1.58	186.8	1.13×10^{-2}	4.48×10^{-2}
bta-let-7e	−1.62	2038.4	4.38×10^{-3}	2.18×10^{-2}
bta-miR-423-5p	−1.64	9504.1	3.95×10^{-4}	3.30×10^{-3}
bta-miR-423-3p	−1.65	9898.1	4.45×10^{-6}	7.83×10^{-5}
bta-let-7a-5p	−1.84	120.9	2.74×10^{-4}	2.69×10^{-3}
bta-miR-345-3p	−1.89	996.2	4.31×10^{-4}	3.43×10^{-3}
bta-let-7b/bta-miR-3596	−1.91	239.4	5.51×10^{-5}	7.16×10^{-4}
bta-miR-128	−1.95	115.8	9.18×10^{-7}	2.55×10^{-5}
bta-let-7c	−2.25	808	4.02×10^{-6}	7.46×10^{-5}
bta-miR-874	−2.85	126	1.37×10^{-15}	2.29×10^{-13}
bta-miR-378b	−4.75	138.1	1.51×10^{-7}	4.60×10^{-6}
bta-miR-296	−4.93	191.8	4.54×10^{-20}	1.52×10^{-17}

FC: fold change; RPM: read per million; FDR: false discovery rate (corrected *P* value).

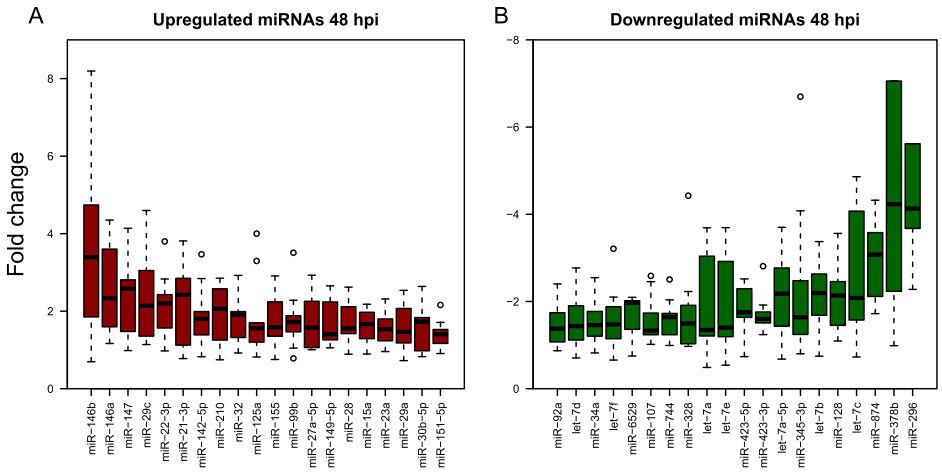

Figure 2. Upregulated (A) and downregulated (B) miRNAs in bovine alveolar macrophages isolated from nine animals at 48 h post-infection with *M. bovis*.

as differentially expressed at 2 hpi (FDR $\leq$ 0.05) (Table 1), while no differentially expressed miRNAs were identified at 6 hpi. Six miRNAs were differentially expressed 24 hpi; of these, five (bta-miR-21-3p, bta-miR-27a-5p, bta-miR-146a, bta-miR-147, and bta-miR-149-5p) were upregulated and one (bta-miR-296) was downregulated (FDR $\leq$ 0.05). Forty differentially expressed miRNAs were identified at 48 hpi (Figure 2), of which 36 had a >1.5 fold change difference in expression. All of the miRNAs that were differentially expressed at 24 hpi were also differentially expressed at 48 hpi. Among the upregulated miRNAs at 48 hpi, bta-miR-146b had the highest fold change (FC = 2.7), followed by bta-miR-146a (FC = 2.4). Seven members of the bta-let-7 family were found to be downregulated post-infection. Interestingly, two highly expressed miRNAs, bta-mir-423-3p, and bta-mir-423-5p, from the opposite arm of the same pre-miRNA, were both downregulated. The full list of differentially expressed miRNAs, their read counts and fold changes are listed in Table 1.

3.2. Validation of three differentially expressed miRNAs using RT-qPCR

The differential expression of four miRNAs (bta-miR-22, bta-miR-142-5p, bta-miR-146a, and bta-miR-423-3p), found to be differentially expressed at 48 hpi using RNA-seq (Supplementary Figure 2), was investigated using reverse transcription quantitative real time PCR (RT-qPCR) in nine biological replicates. Differential expression was confirmed in three out of the four cases: miR-142-5p (FC = 1.3), miR-146a (FC = 3.0), and miR-423-3p (FC = −1.7). The upregulation of miR-22 (FC = 1.1) was not statistically significant (Figure 3). For the efficiency corrected C_t values for each sample, see Supplementary Table 5.

3.3. Two potentially novel bovine miRNAs are predicted from the sequencing data

Using miRDeep2, two putatively novel bovine miRNAs were identified from the sequencing data: bta-mir-10225a (mature sequence: ccgagccugacagaucacaca), located on chromosome 26, was found to be expressed in all animals (in 52 samples in total, with no preference for timepoint or infection status), with a mean expression of 1890 RPM. A close homolog (with just one nucleotide mismatch) was also predicted in an adjacent genomic region (bta-mir-10225b; mature sequence: ucgagccugacagaucacaca), and was detected in six animals (13 samples) with a mean expression of 950 RPM. There are several near-identical copies of these miRNAs in the same region.

3.4. The predicted targets of upregulated miRNAs are enriched for roles in endocytosis and lysosome function

To identify the potential mRNA targets of differentially expressed miRNAs, we identified those mRNAs with expression values (from Nalpas et al., manuscript submitted) significantly negatively correlated with miRNA expression. These predictions were further refined by removing those miRNA-target predicted relationships that were not supported by a predicted miRNA seed region match in the 3′ UTR of the correlated mRNA (Figure 4A, Supplementary Table 6). This network of miRNA-mRNA interactions was visualized with Cytoscape (Figure 4B). It is apparent that miR-22-3p, miR-146a and b, miR-147, and miR-155 share many targets, suggesting they have a common role. Among the downregulated miRNAs, the let-7 family members, and miR-423-3p and -5p share most of their targets.

Analysis of the predicted target genes using InnateDB (www.innatedb.com) [22], revealed that the predicted targets of upregulated miRNAs were highly enriched for roles in the lysosome

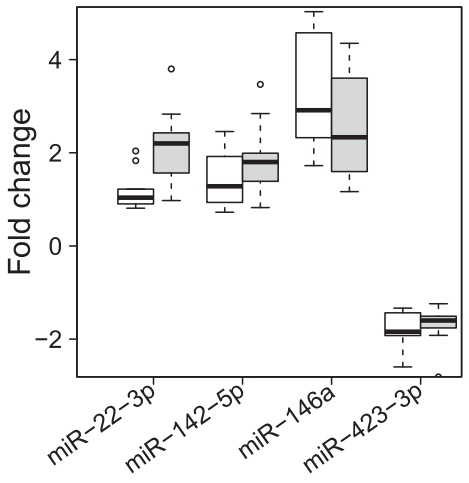

Figure 3. The differential expression of three (bta-miR-142-5p, bta-miR-146a, and bta-miR-423-3p) out of four miRNAs for the nine animals at 48 hpi was confirmed with RT-qPCR (white). RNA-seq fold changes for these miRNAs are also shown (light grey).

(FDR $\leq 3.2 \times 10^{-6}$) and in endocytosis (FDR ≤ 0.02). Key components of innate immunity signalling pathways, including the Toll-like receptor (TLR) pathway, transforming growth factor beta receptor (TGFBR) signalling pathway, and the IL-10 anti-inflammatory signalling pathway, were also predicted to be preferentially targeted by upregulated miRNAs (Supplementary Table 7).

In comparison, downregulated miRNAs were predicted to preferentially target IL-1 (FDR $\leq 5.4 \times 10^{-6}$) and MAPK signalling (FDR = 0.0001) pathways, as well as the tumour necrosis factor receptor 1 (TNFR1) signalling pathway (FDR ≤ 0.03) and genes involved in bacterial invasion (Supplementary Table 7). Additionally, the Toll-like receptor pathway was also targeted by downregulated miRNAs. Of the 22 TLR pathway genes predicted to be targeted, 11 were predicted to be targeted only by downregulated miRNAs, and 7 only by upregulated miRNAs.

3.5. Overexpression of miR-146 results in the transcriptional suppression of IRAK1 and TGFBR2

We have utilized a miRNA overexpression strategy to validate the predicted post-transcriptional regulation of two genes in these pathways by miR-146, a microRNA shown by RNA-seq and RT-qPCR to be upregulated in response to *M. bovis* infection. Successful transfection of miRNA mimics into a bovine macrophage cell line (Bomac) was confirmed by the positive control miR-1, which was observed to three-fold downregulate its target, *PTK9*. In contrast, miR-1 did not alter the expression of *IRAK1,* and only marginally (1.2 fold upregulation) altered *TGFBR2* mRNA levels (Supplementary Table 3). miR-146a or miR-146b was predicted from our computational analyses to downregulate *IRAK1*, and indeed, transfection (i.e. overexpression) of miRNA mimics for these miRNAs into Bomacs led to a more than three-fold suppression of *IRAK1* transcription (Figure 5), a central kinase in the TLR and IL-1 pathways [28]. Another predicted target of bta-miR-146a and bta-miR-146b, *TGFBR2,* which is part of the TGF-β receptor pathway, was also downregulated 1.5 fold upon transfection with mimics (Figure 5).

4. Discussion

In this study, we have used high-throughput sequencing to profile miRNA expression at multiple time-points, in primary bovine alveolar macrophages infected with *M. bovis*, the causative agent of bovine TB. Over the time-course, 41 miRNAs were identified as being significantly differentially expressed in response to *M. bovis* infection. The majority of miRNAs were differentially expressed only after 48 hpi. Several of the differentially expressed miRNAs have been shown to have regulatory roles in monocytes and macrophages and during infection. For example, miR-149-5p, which was upregulated in our study at 24 and 48 hpi, has also been shown to be upregulated in murine bone-marrow derived macrophages infected with *Listeria monocytogenes* [29]. Another highly expressed miRNA detected in our study, miR-27, has previously been shown to have a role in the activation of human macrophages [30,31].

Many of the differentially expressed miRNAs have also been shown to have a role in other mycobacterial infections. The most highly expressed miRNA at 24 hpi, bta-miR-146a, was upregulated more than two-fold, and has also been found to be upregulated in human MDMs after *M. avium* infection [10]. Another example at 24 hpi is bta-miR-21-3p. MiR-21 has a well-established role in immunity and has been shown to target the vitamin D-dependent antimicrobial pathway in *Mycobacterium leprae* infected monocytes [32,33]. MicroRNAs bta-mir-423-3p, and bta-mir-423-5p, which were downregulated in response to *M. bovis* infection in our study, have also been found to be downregulated in human MDM infected with *M. avium* [10], and are involved in regulating chemokine expression and apoptosis related pathways. Although these findings show that not all observed changes are *M. bovis*-specific, the differentially expressed miRNAs may serve as potential biomarker

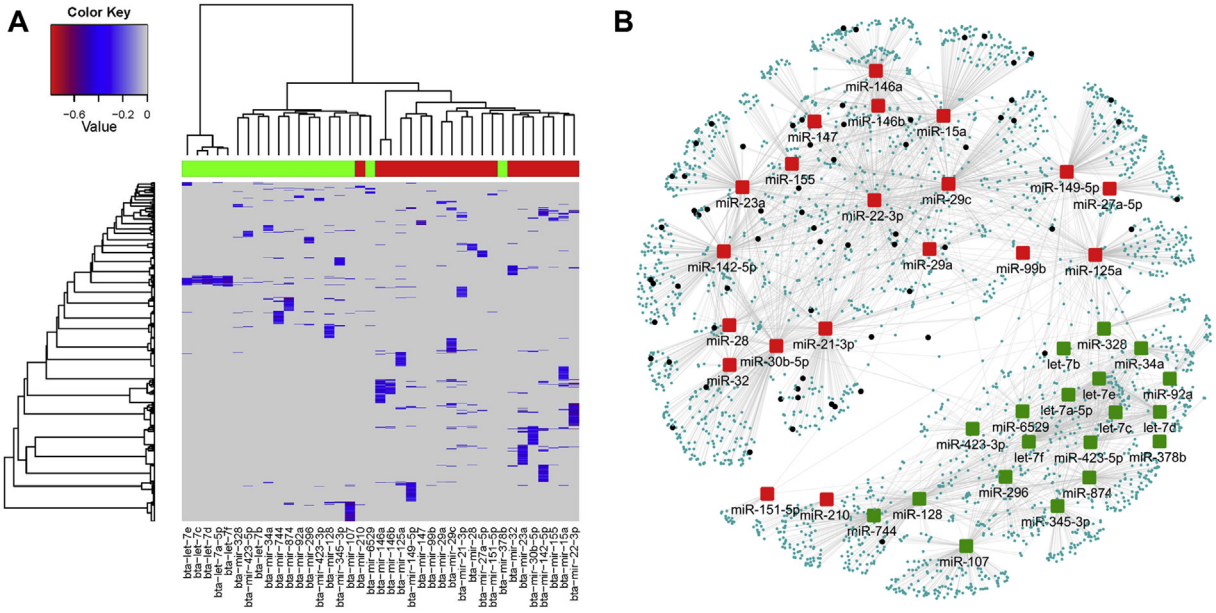

Figure 4. A) Two-dimensional cluster analysis and heatmap visualization of significant correlations (shown as coloured lines) between miRNA and mRNA expression at 48 hpi. Non-significant correlations and those not supported by a 3′ UTR miRNA seed match are shown in grey. Please see the colour key in the figure. The primary split in the upper hierarchical dendrogram largely aligns with the upregulated (red) and downregulated miRNAs (green). B) A network of the predicted mRNA targets of differentially expressed miRNAs at 48 hpi with *M. bovis*. Targets are predicted based on a significant negative correlation between miRNA and mRNA expression and the presence of a miR and a seed match in the correlated mRNA. Squares = miRNAs; Circles = mRNAs. Red = upregulated; Green = downregulated. Lysosome and endocytosis pathway genes are shown as black circles. Please see Supplementary Table 6 for details of targeted mRNAs.

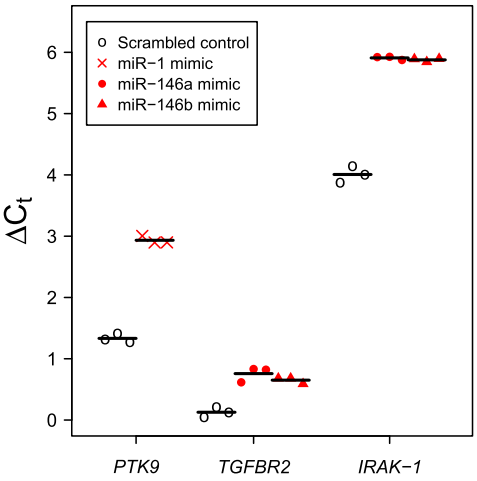

Figure 5. Transfection of miRNA mimics for miR-146a or miR-146b into a bovine macrophage cell line (Bomac) led to a 3 fold suppression of IRAK1 transcription, and a 1.5 fold downregulation of TGFBR2 in comparison to a scrambled control miRNA, as measured by RT-qPCR. Successful transfection was confirmed by the positive control miR-1, which was observed to downregulate its target, PTK9, by 3 fold.

candidates for *M. bovis* infection in cattle, for example, as was suggested for miR-155 [34].

Pathway analysis of the predicted mRNA targets of DE miRNAs suggests that these miRNAs preferentially target several pathways that are functionally relevant for mycobacterial pathogenesis. The predicted targets of upregulated miRNAs at 48 hpi, for example, were statistically enriched for functions in the lysosome and in the endocytosis pathway. These pathways were predicted to be targeted by multiple miRNAs including bta-miR-15a, bta-miR-21-3p, bta-miR-22-3p, bta-miR-23a, bta-miR-30b-5p and bta-miR-142-5p. A key feature of mycobacteria is their ability to survive and reproduce in the phagosome by retarding maturation of the phagosome along the endosomal-lysosomal pathway and blocking fusion with the lysosome [35]. Mycobacteria also enhance phagosome fusion with early endosomes, possibly providing access to host nutrients and secreted glycoproteins [36]. In our analysis, the endocytosis pathway was predicted to be targeted mainly through several members of the membrane trafficking regulator Rab family, namely, RAB22A, RAB4A, RAB5B, RAB5C, and RAB7A, in addition to rabaptin (RABEP1) and the RAB11 family interacting protein 5 (RAB11FIP5). Autophagy is an effective innate defence mechanism for eliminating mycobacteria [37,38]. Recently, the Rab protein family was found to be necessary for autophagic clearance of mycobacteria and the knockdown of Rab proteins resulted in increased *M. bovis*-BCG survival [39]. Our results therefore suggest that *M. bovis* utilizes host miRNAs as part of its strategy to manipulate these processes for its own benefit and survival.

We have also shown, that overexpression of miR-146a and miR-146b, which are upregulated during *M. bovis* infection, leads to a downregulation of *IRAK1,* a central kinase in IL-1 signal transduction [40], TLR signalling and in the Type I Interferon Pathway [41]. The targeting of IRAK1 by miR-146a/b has also been demonstrated in human [42] and mouse [43]. IL-1 receptor signalling is required for the innate response to *M. tuberculosis* and IL1R1-deficient mice display a dramatic defect of early control of MTB infection [44]. Thus, this may be another example of *M. bovis* exploiting host miRNAs for its own benefit. Pathway analysis, however, has also revealed that despite the targeting of IRAK1 by upregulated miR-146a/b, many other members of this pathway were statistically enriched as targets of downregulated miRNAs, which would be predicted to transcriptionally upregulate these genes in the IL-1 pathway. This suggests that both the pathogen and the host are battling for the control of this central pro-inflammatory pathway at the post-transcriptional level.

The transforming growth factor beta (TGF-β) pathway was also predicted to be significantly targeted by upregulated miRNAs and we have shown that the overexpression of miR-146a or miR-146b – two of the upregulated miRNAs – results in the downregulation of TGFBR2, one the receptors for the TGF-β pathway. TGF-β signalling has a well-established role in tuberculosis pathogenesis [45]. Thus, the post-transcriptional targeting of this pathway by upregulated miRNAs may be an example of the host immune response utilizing miRNAs for the benefit of the host.

In conclusion, our work, which investigates the post-transcriptional regulation of the innate immune response by miRNAs in alveolar macrophages, the natural host cell-type for *M. bovis*, suggests that miRNAs play a key role in finely tuning the complex interplay and tightly controlled balance between pathogen survival strategies and the host immune response.

Funding: This project was funded by Teagasc (RMIS 6082), an Investigator Grant from Science Foundation Ireland (SFI/08/IN.1/B2038), and a Research Stimulus Grant from the Department of Agriculture, Food and the Marine (RSF 06 405). Peter Vegh is supported by a Teagasc Walsh Fellowship.

Competing interests: The authors have no conflict of interest to declare.

Ethical approval: All animal procedures were performed in accordance with the provisions of the Irish Cruelty to Animals Act, and ethical approval for the study was obtained from the University College Dublin Animal Ethics Committee (protocol number AREC-13-14-Gordon).

Acknowledgements

We thank Prof. Cliona O'Farrelly (Trinity College Dublin) for the Bomac cells. We thank Dr. Eddie Jordan (UCD Lyons Research Farm), Dr. Joseph Cassidy, Mr. Brian Cloak, Ms. Claire Healy, Ms. Kirsten McLoughlin and Ms. Jing Chen (all UCD College of Agriculture, Food Science and Veterinary Medicine) for assistance with animal procurement and lung lavages. We also thank Dr. George Cloughley, Ms. Bernadette Legget, Mrs. Yvonne Abbott and Mrs. Maureen McCullough for assistance with microbial testing of samples (all UCD College of Agriculture, Food Science and Veterinary Medicine).

Appendix A. Supplementary data

Supplementary data related to this article can be found at http://dx.doi.org/10.1016/j.tube.2014.10.011.

References

[1] WHO. Global tuberculosis report. 2013.
[2] Ehlers S. Lazy, dynamic or minimally recrudescent? On the elusive nature and location of the mycobacterium responsible for latent tuberculosis. Infection 2009;37:87–95.
[3] Subbian S, Bandyopadhyay N, Tsenova L, O'Brien P, Khetani V, Kushner NL, Peixoto B, Soteropoulos P, Bader JS, Karakousis PC, Fallows D, Kaplan G. Early innate immunity determines outcome of mycobacterium tuberculosis pulmonary infection in rabbits. Cell Commun Signal 2013;11:60.
[4] Magee DA, Taraktsoglou M, Killick KE, Nalpas NC, Browne JA, Park SD, Conlon KM, Lynn DJ, Hokamp K, Gordon SV, Gormley E, MacHugh DE. Global gene expression and systems biology analysis of bovine monocyte-derived macrophages in response to in vitro challenge with *Mycobacterium bovis*. PLoS One 2012;7:e32034.
[5] Nalpas NC, Park SD, Magee DA, Taraktsoglou M, Browne JA, Conlon KM, Rue-Albrecht K, Killick KE, Hokamp K, Lohan AJ, Loftus BJ, Gormley E, Gordon SV,

Machugh DE. Whole-transcriptome, high-throughput RNA sequence analysis of the bovine macrophage response to *Mycobacterium bovis* infection in vitro. BMC Genomics 2013;14:230.
[6] Holley CL, Topkara VK. An introduction to small non-coding RNAs: miRNA and snoRNA. Cardiovasc Drugs Therapy – Sponsored Int Soc Cardiovasc Pharmacother 2011;25:151–9.
[7] Gantier MP. New perspectives in microRNA regulation of innate immunity. J Interferon Cytokine Res 2010;30:283–9.
[8] Singh PK, Singh AV, Chauhan DS. Current understanding on micro RNAs and its regulation in response to mycobacterial infections. J Biomed Sci 2013;20:14.
[9] Ma F, Xu S, Liu X, Zhang Q, Xu X, Liu M, Hua M, Li N, Yao H, Cao X. The microRNA mir-29 controls innate and adaptive immune responses to intracellular bacterial infection by targeting interferon-gamma. Nat Immunol 2011;12:861–9.
[10] Sharbati J, Lewin A, Kutz-Lohroff B, Kamal E, Einspanier R, Sharbati S. Integrated microRNA-mRNA-analysis of human monocyte derived macrophages upon mycobacterium avium subsp. Hominissuis infection. PLoS One 2011;6:e20258.
[11] Vegh P, Foroushani AB, Magee DA, McCabe MS, Browne JA, Nalpas NC, Conlon KM, Gordon SV, Bradley DG, MacHugh DE, Lynn DJ. Profiling microRNA expression in bovine alveolar macrophages using RNA-seq. Vet Immunol Immunopathol 2013;155:238–44.
[12] Magee DA, Conlon KM, Nalpas NC, Browne JA, Pirson C, Healy C, McLoughlin KE, Chen J, Vordermeier HM, Gormley E, MacHugh DE, Gordon SV. Innate cytokine profiling of bovine alveolar macrophages reveals commonalities and divergence in the response to *Mycobacterium bovis* and *Mycobacterium tuberculosis* infection. Tuberc – Edinb 2014;94(4):441–50.
[13] Barrett T, Troup DB, Wilhite SE, Ledoux P, Evangelista C, Kim IF, Tomashevsky M, Marshall KA, Phillippy KH, Sherman PM, Muertter RN, Holko M, Ayanbule O, Yefanov A, Soboleva A. Ncbi geo: archive for functional genomics data sets–10 years on. Nucleic Acids Res 2011;39:D1005–10.
[14] Martin M. Cutadapt removes adapter sequences from high-throughput sequencing reads. 2011.
[15] Zimin AV, Delcher AL, Florea L, Kelley DR, Schatz MC, Puiu D, Hanrahan F, Pertea G, Van Tassell CP, Sonstegard TS, Marcais G, Roberts M, Subramanian P, Yorke JA, Salzberg SL. A whole-genome assembly of the domestic cow, bos taurus. Genome Biol 2009;10:R42.
[16] Kozomara A, Griffiths-Jones S. Mirbase: integrating microRNA annotation and deep-sequencing data. Nucleic Acids Res 2011;39:D152–7.
[17] Friedlander MR, Chen W, Adamidi C, Maaskola J, Einspanier R, Knespel S, Rajewsky N. Discovering micrornas from deep sequencing data using mirdeep. Nat Biotechnol 2008;26:407–15.
[18] Robinson MD, McCarthy DJ, Smyth GK. Edger: a bioconductor package for differential expression analysis of digital gene expression data. Bioinformatics 2010;26:139–40.
[19] Garmire LX, Subramaniam S. Evaluation of normalization methods in mammalian microRNA-seq data. RNA 2012;18:1279–88.
[20] Mullokandov G, Baccarini A, Ruzo A, Jayaprakash AD, Tung N, Israelow B, Evans MJ, Sachidanandam R, Brown BD. High-throughput assessment of microRNA activity and function using microRNA sensor and decoy libraries. Nat Methods 2012;9:840–6.
[21] Cline MS, Smoot M, Cerami E, Kuchinsky A, Landys N, Workman C, Christmas R, Avila-Campilo I, Creech M, Gross B, Hanspers K, Isserlin R, Kelley R, Killcoyne S, Lotia S, Maere S, Morris J, Ono K, Pavlovic V, Pico AR, Vailaya A, Wang PL, Adler A, Conklin BR, Hood L, Kuiper M, Sander C, Schmulevich I, Schwikowski B, Warner GJ, Ideker T, Bader GD. Integration of biological networks and gene expression data using cytoscape. Nat Protoc 2007;2:2366–82.
[22] Lynn DJ, Winsor GL, Chan C, Richard N, Laird MR, Barsky A, Gardy JL, Roche FM, Chan TH, Shah N, Lo R, Naseer M, Que J, Yau M, Acab M, Tulpan D, Whiteside MD, Chikatamarla A, Mah B, Munzner T, Hokamp K, Hancock RE, Brinkman FS. InnateDB: facilitating systems-level analyses of the mammalian innate immune response. Mol Syst Biol 2008;4:218.
[23] Benjamini Y, Hochberg Y. Controlling the false discovery rate: a practical and powerful approach to multiple testing. J R Stat Soc Ser B Methodol 1995;57:289–300.
[24] Pfaffl MW. A new mathematical model for relative quantification in real-time RT-PCR. Nucleic Acids Res 2001;29:e45.
[25] Sager H, Davis WC, Jungi TW. Bovine monocytoid cells transformed to proliferate cease to exhibit lineage-specific functions. Vet Immunol Immunopathol 1999;68:113–30.
[26] Vandesompele J, De Preter K, Pattyn F, Poppe B, Van Roy N, De Paepe A, Speleman F. Accurate normalization of real-time quantitative RT-PCR data by geometric averaging of multiple internal control genes. Genome Biol 2002;3.RESEARCH0034.
[27] Perkins JR, Dawes JM, McMahon SB, Bennett DL, Orengo C, Kohl M. ReadqPCR and normqPCR: R packages for the reading, quality checking and normalisation of RT-qPCR quantification cycle (cq) data. BMC Genomics 2012;13:296.
[28] O'Neill LA. The interleukin-1 receptor/toll-like receptor superfamily: 10 years of progress. Immunol Rev 2008;226:10–8.
[29] Schnitger AKD, Machova A, Mueller RU, Androulidaki A, Schermer B, Pasparakis M, Krönke M, Papadopoulou N. *Listeria monocytogenes* infection in macrophages induces vacuolar-dependent host miRNA response. PLoS One 2011;6:e27435.
[30] Cheng Y, Kuang W, Hao Y, Zhang D, Lei M, Du L, Jiao H, Zhang X, Wang F. Downregulation of mir-27a* and mir-532-5p and upregulation of mir-146a and mir-155 in LPS-induced raw264.7 macrophage cells. Inflammation 2012;35:1308–13.
[31] Graff JW, Dickson AM, Clay G, McCaffrey AP, Wilson ME. Identifying functional microRNAs in macrophages with polarized phenotypes. J Biol Chem 2012;287:21816–25.
[32] Liu PT, Wheelwright M, Teles R, Komisopoulou E, Edfeldt K, Ferguson B, Mehta MD, Vazirnia A, Rea TH, Sarno EN, Graeber TG, Modlin RL. MicroRNA-21 targets the vitamin d-dependent antimicrobial pathway in leprosy. Nat Med 2012;18:267–73.
[33] O'Neill LA, Sheedy FJ, McCoy CE. Micrornas: the fine-tuners of toll-like receptor signalling. Nat Rev Immunol 2011;11:163–75.
[34] Golby P, Villarreal-Ramos B, Dean G, Jones GJ, Vordermeier M. MicroRNA expression profiling of PPD-B stimulated PBMC from *M. Bovis*-challenged unvaccinated and BCG vaccinated cattle. Vaccine 2014;32:5839–44.
[35] Clemens DL, Horwitz MA. Characterization of the mycobacterium tuberculosis phagosome and evidence that phagosomal maturation is inhibited. J Exp Med 1995;181:257–70.
[36] Vergne I, Fratti RA, Hill PJ, Chua J, Belisle J, Deretic V. *Mycobacterium tuberculosis* phagosome maturation arrest: *Mycobacterial phosphatidylinositol* analog phosphatidylinositol mannoside stimulates early endosomal fusion. Mol Biol Cell 2004;15:751–60.
[37] Ni Cheallaigh C, Keane J, Lavelle EC, Hope JC, Harris J. Autophagy in the immune response to tuberculosis: clinical perspectives. Clin Exp Immunol 2011;164:291–300.
[38] Deretic V, Delgado M, Vergne I, Master S, De Haro S, Ponpuak M, Singh S. Autophagy in immunity against *Mycobacterium tuberculosis*: a model system to dissect immunological roles of autophagy. Curr Top Microbiol Immunol 2009;335:169–88.
[39] Pilli M, Arko-Mensah J, Ponpuak M, Roberts E, Master S, Mandell MA, Dupont N, Ornatowski W, Jiang S, Bradfute SB, Bruun JA, Hansen TE, Johansen T, Deretic V. TBK-1 promotes autophagy-mediated antimicrobial defense by controlling autophagosome maturation. Immunity 2012;37:223–34.
[40] Liu G, Park YJ, Abraham E. Interleukin-1 receptor-associated kinase (IRAK) -1-mediated NF-kappab activation requires cytosolic and nuclear activity. FASEB J – Off Publ Fed Am Soc Exp Biol 2008;22:2285–96.
[41] Pauls E, Nanda SK, Smith H, Toth R, Arthur JS, Cohen P. Two phases of inflammatory mediator production defined by the study of IRAK2 and IRAK1 knock-in mice. J Immunol 2013;191:2717–30.
[42] Taganov KD, Boldin MP, Chang KJ, Baltimore D. NF-kappaB-dependent induction of microRNA mir-146, an inhibitor targeted to signaling proteins of innate immune responses. Proc Natl Acad Sci U S A 2006;103:12481–6.
[43] Hou J, Wang P, Lin L, Liu X, Ma F, An H, Wang Z, Cao X. MicroRNA-146a feedback inhibits RIG-I-dependent type I IFN production in macrophages by targeting TRAF6, IRAK1, and IRAK2. J Immunol 2009;183:2150–8.
[44] Fremond CM, Togbe D, Doz E, Rose S, Vasseur V, Maillet I, Jacobs M, Ryffel B, Quesniaux VF. Il-1 receptor-mediated signal is an essential component of myd88-dependent innate response to *Mycobacterium tuberculosis* infection. J Immunol 2007;179:1178–89.
[45] Toossi Z, Ellner JJ. The role of TGF beta in the pathogenesis of human tuberculosis. Clin Immunol Immunopathol 1998;87:107–14.